

# Normalizing Flows for Gaussian Process Regression under Hierarchical Shrinkage Priors

Peter Knaus\*

**Abstract.** Gaussian Process Regression (GPR) is a powerful tool for nonparametric regression, but its fully Bayesian application in high-dimensional settings is hindered by two primary challenges: the computational burden (exacerbated by fully Bayesian inference) and the difficulty of variable selection. This paper introduces a novel methodology that combines hierarchical global-local shrinkage priors with normalizing flows to address these challenges. The hierarchical triple gamma prior offers a principled framework for inducing sparsity in high-dimensional GPR, effectively excluding irrelevant covariates while preserving interpretability and flexibility in model size. Normalizing flows are employed within a variational inference framework to approximate the posterior distribution of hyperparameters, capturing complex dependencies while ensuring computational scalability. Simulation studies demonstrate the efficacy of the proposed approach, outperforming traditional maximum likelihood estimation and mean-field variational methods, particularly in high-sparsity and high-dimensional settings. The results highlight the robustness and flexibility of hierarchical shrinkage priors and the computational efficiency of normalizing flows for Bayesian GPR. This work provides a scalable and interpretable solution for high-dimensional regression, with implications for sparse modeling and posterior approximation in broader Bayesian contexts.

**MSC2020 subject classifications:** Primary 62G08, 62F15; secondary 62H12, 60G15.

**Keywords:** Variational inference, Variable selection, Covariance shrinkage, Triple gamma shrinkage prior.

## 1 Introduction

Gaussian process regression (GPR) is a widely used tool in nonparametric regression, valued for its theoretical rigor—achieving near-minimax rates of convergence to the true underlying function (van der Vaart and van Zanten, 2009)—all while retaining interpretability. However, two major challenges arise in practice. First, selecting the hyperparameters that govern the covariance structure becomes increasingly complex as the number of predictors grows, requiring variable selection to distinguish influential covariates from noise. Second, estimating GPR models, particularly within a fully Bayesian framework, is computationally demanding. The cost of evaluating the likelihood scales cubically with the number of observations, making standard approaches like Markov chain Monte Carlo (MCMC) prohibitively expensive for large datasets.

Several methods have been proposed for variable selection in GPR. The most well-known is automatic relevance determination (ARD) by Neal (1996), which identifies

---

\*Department of Statistics, Harvard University, [pknaus@fas.harvard.edu](mailto:pknaus@fas.harvard.edu)

covariate importance through maximum-likelihood hyperparameter estimates but lacks explicit sparsity. Penalized approaches, such as those by [Yan and Qi \(2010\)](#) and [Yi et al. \(2011\)](#), address this by enforcing sparsity directly, for example, through the  $\ell_1$  penalty. Alternatively, sensitivity-based methods (e.g., [Piironen and Vehtari, 2016](#); [Paananen et al., 2019](#)) evaluate the predictive changes when covariates are removed, while dimension-reduction techniques (e.g., [Park et al., 2022](#); [Tripathy et al., 2016](#); [Liu and Guillas, 2017](#)) focus on finding lower-dimensional representations of the covariates, often at the expense of interpretability.

Despite being couched in Bayesian terminology, all previously mentioned methods for variable selection in GPR are not fully Bayesian, as they yield only point estimates for hyperparameters and lack the full uncertainty quantification inherent to Bayesian analysis. This limitation can result in overconfidence in predictions and reduced out-of-sample performance. Fully Bayesian approaches, while less common, aim to address this. For example, [Chen and Wang \(2010\)](#) and [Savitsky et al. \(2011\)](#) use spike-and-slab priors ([Mitchell and Beauchamp, 1988](#); [George and McCulloch, 1993, 1997](#)) to induce sparsity, providing posterior inclusion probabilities for each covariate. However, these methods become computationally expensive in higher dimensions. Others, such as [Vo and Pati \(2017\)](#), adopt computationally tractable alternatives like the horseshoe prior ([Carvalho et al., 2010](#)) to induce sparsity in additive GPR frameworks. More recently, [Tang et al. \(2024\)](#) applied cumulative shrinkage priors ([Legramanti et al., 2020](#)) using the Karhunen-Loève decomposition ([Alexanderian, 2015](#)), which embeds a hierarchy of effects but sacrifices interpretability.

While theoretically more attractive, fully Bayesian approaches face a significant computational hurdle, particularly in high-dimensional GPR settings, due to the cubic scaling of the likelihood evaluation with the number of observations. Sampling-based methods such as MCMC exacerbate this issue, as they require repeated likelihood evaluations. For example, single-move Metropolis-Hastings updates each parameter sequentially, making high-dimensional applications infeasible. Even more efficient samplers, like Hamiltonian Monte Carlo (HMC), can remain prohibitive due to the computational cost of evaluating gradients at each leapfrog step. Variational inference (VI) offers a potential solution by reducing computational demands, but many widely used VI implementations rely on mean-field approximations. This reliance limits expressivity, making it challenging to accurately capture complex posterior distributions and often leading to suboptimal results. These computational challenges constrain the applicability of fully Bayesian GPR to small datasets.

In this paper, I tackle the two aforementioned problems simultaneously. Recent insights from the hierarchical global-local shrinkage literature are introduced into the GPR framework, providing an interpretable and flexible approach to variable selection. Additionally, normalizing flows ([Rezende and Mohamed, 2015](#)) are employed within a variational inference framework to flexibly approximate the posterior distribution of the hyperparameters, capturing dependencies in the posterior while ensuring scalability and maintaining proper uncertainty quantification. Together, these advances enable a principled Bayesian approach to variable selection, yielding interpretable models that remain computationally tractable in higher dimensions.

The remainder of this paper is structured as follows. Section 2 introduces hierarchical global-local shrinkage priors for GPR. Section 3 provides an overview of normalizing flows and how they can be used to approximate the posterior distribution of the hyperparameters. Section 4 presents a simulation study to assess the performance of the proposed method. Section 5 applies the method to a real data set. Finally, Section 6 concludes.

## 2 Hierarchical Shrinkage in Gaussian Process Regression

This work considers the following multivariate nonparametric regression framework

$$y_i = f(\mathbf{x}_i) + \epsilon_i, \quad (1)$$

where  $f$  is an unknown mean regression function to be estimated from the data  $\mathcal{D} = \{(\mathbf{x}_i, y_i)\}_{i=1}^N$ , which in turn consists of the covariates  $\mathbf{x}_i \in \mathbb{R}^d$  and the responses  $y_i \in \mathbb{R}$ , and  $\epsilon_i \sim \mathcal{N}(0, \sigma^2)$  is the noise term. The regression function  $f$  is placed under a Gaussian Process (GP) prior with a zero mean function (a choice that can be relaxed if needed). The GP prior is defined as

$$f \mid \boldsymbol{\zeta}, \mathbf{x} \sim \mathcal{GP}(0, k(\mathbf{x}, \mathbf{x}'; \boldsymbol{\zeta})), \quad (2)$$

where  $k(\mathbf{x}, \mathbf{x}'; \boldsymbol{\zeta})$  is a positive definite kernel function that depends on the hyperparameters  $\boldsymbol{\zeta}$ . Under this specification, marginalizing over the latent function  $f$  yields the prior joint distribution of the response vector  $\mathbf{y}$ , incorporating both the covariance structure and noise term:

$$\mathbf{y} \mid \boldsymbol{\zeta}, \mathbf{x}, \sigma^2 \sim \mathcal{N}(0, \mathbf{K}(\mathbf{x}; \boldsymbol{\zeta}) + \sigma^2 \mathbf{I}), \quad (3)$$

where the covariance matrix  $\mathbf{K}(\mathbf{x}; \boldsymbol{\zeta})$  is defined elementwise as  $\mathbf{K}(\mathbf{x}; \boldsymbol{\zeta})_{ij} = k(\mathbf{x}_i, \mathbf{x}_j; \boldsymbol{\zeta})$  (Rasmussen and Williams, 2005).

Many choices are feasible for the covariance function  $k(\mathbf{x}, \mathbf{x}'; \boldsymbol{\zeta})$ . Examples include the squared exponential kernel, the Matérn kernel, the rational quadratic kernel, or the periodic kernel. While these differ in characteristics like implied smoothness, correlation between "distant" observations, or periodicity, many of them — when used in the context of regression — have at their core an anisotropic distance function of the form

$$\delta(\mathbf{x}, \mathbf{x}'; \boldsymbol{\theta}) = \sqrt{\sum_{j=1}^d (x_j - x'_j)^2 \theta_j}, \quad (4)$$

where  $\theta_j$  determines the contribution of  $j$ -th covariate to the distance. Consider, as an example, the squared exponential kernel written in this way:

$$k_{SE}(\mathbf{x}, \mathbf{x}'; \tau, \boldsymbol{\theta}) = \frac{1}{\tau} \exp\left(-\frac{1}{2} \delta(\mathbf{x}, \mathbf{x}'; \boldsymbol{\theta})^2\right). \quad (5)$$

where  $\tau$  determines the overall variance of the Gaussian process. The hyperparameters  $\boldsymbol{\theta}$  dictate how each covariate contributes to the distance function, directly influencing the

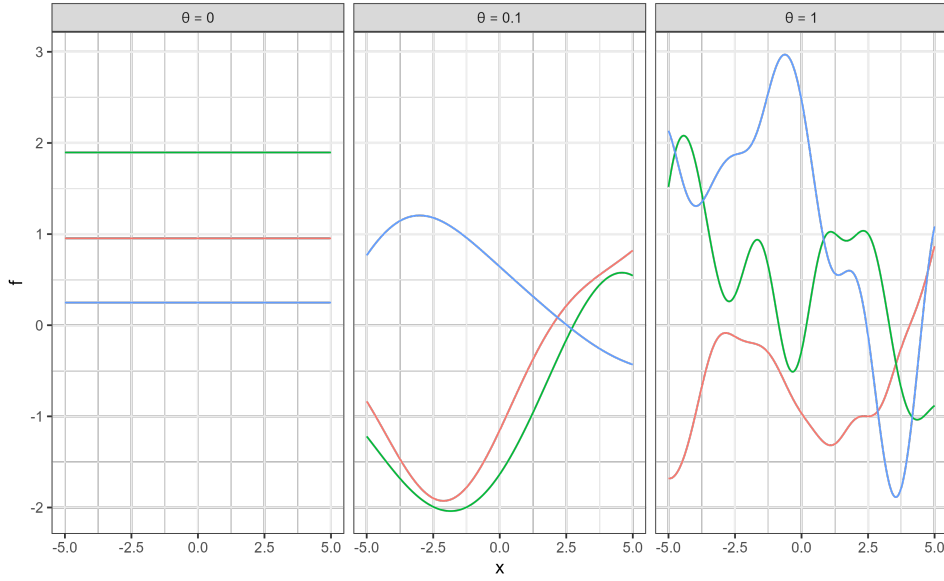


Figure 1: Samples from a Gaussian process with a squared exponential kernel, with varying values of  $\theta_j$ . As  $\theta_j$  becomes smaller, the draws become smoother, with the extreme case of  $\theta_j = 0$  leading to a constant function.

covariance structure of the Gaussian process. As  $\theta_j$  becomes small, the  $j$ -th covariate contributes less to the distance function, resulting in reduced influence on the covariance structure. In the limit, when  $\theta_j = 0$ , the  $j$ -th covariate no longer affects the covariance structure and can be considered irrelevant. This effect is clearly illustrated in Figure 1, which shows realizations from a Gaussian process with varying  $\theta_j$  values. Smaller values of  $\theta_j$  result in smoother functions, while  $\theta_j = 0$  leads to a constant function, where the covariate has no more influence on the outcome. Notably, the covariance structure is governed by only a handful of hyperparameters, which simplifies the estimation process discussed in Section 3. Despite this simplicity, the Gaussian process retains high flexibility, making it suitable for modeling complex relationships.

When  $d$  is large, i.e., when one is faced with many potential predictors, a mechanism is required to remove irrelevant covariates from the model. In high-dimensional settings, it is often the case that many covariates are irrelevant, contributing noise rather than predictive value. Removing these covariates improves both interpretability and statistical efficiency while safeguarding predictive performance. In the more traditional linear regression setting, this is a well-studied problem, with a popular Bayesian approach being global-local shrinkage priors (Polson and Scott, 2011):

$$\beta_j \mid \tau, \lambda_j \sim \mathcal{N}(0, \tau \lambda_j), \quad \lambda_j \sim \pi_\lambda(\lambda_j), \quad \tau \sim \pi_\tau(\tau), \quad (6)$$

where  $\beta_j$  is the regression coefficient for the  $j$ -th covariate,  $\lambda_j$  is the local shrinkage parameter, and  $\tau$  is the global shrinkage parameter. The idea behind these priors is that

$\tau$  pulls all  $\beta_j$  towards zero, while local parameters  $\lambda_j$  allow select  $\beta_j$  to remain non-zero if supported by the data. Such priors are hierarchical in nature, with the global parameter  $\tau$  inducing a joint distribution that shares information across coefficients and enables adaptation to varying sparsity levels. Various choices of  $\pi_\lambda(\lambda_j)$  and  $\pi_\tau(\tau)$  have been studied in the literature, such as the normal-gamma prior (Griffin and Brown, 2010), the Bayesian Lasso (Park and Casella, 2008), the horseshoe prior (Carvalho et al., 2009) or the triple gamma prior (Cadonna et al., 2020), to name a few.

In their default specification, global-local shrinkage priors are not directly applicable to the GPR framework, as they are defined for regression coefficients with support on  $\mathbb{R}$ . In contrast, the parameters that govern the covariance structure in GPR,  $\theta_1, \dots, \theta_d$ , must remain positive to ensure a valid distance function and meaningful covariance structure. To address this, this work adopts the approach of Frühwirth-Schnatter and Wagner (2010), which is well-established in the time-varying parameter literature, and sets  $\theta_j = \beta_j^2$ . This transformation replaces the normal distribution at the lowest level of the hierarchy with a gamma distribution:

$$\theta_j \mid \tau, \lambda_j \sim \mathcal{G}\left(\frac{1}{2}, \frac{1}{2\tau\lambda_j}\right), \quad \lambda_j \sim \pi_\lambda(\lambda_j), \quad \tau \sim \pi_\tau(\tau), \quad (7)$$

which defines a class of positive shrinkage priors, while retaining the global-local structure, enabling shared shrinkage across parameters via  $\tau$  and flexibility for individual  $\theta_j$  through  $\lambda_j$ .

This work specifically considers the hierarchical triple gamma prior of Cadonna et al. (2020) for  $\theta_j$ , which is well-suited for high-dimensional GPR due to its flexibility, generality, and computational tractability. While the triple gamma prior is traditionally represented as a compound distribution of three gamma random variables, its global-local form closest to (7) is given by

$$\theta_j \mid \tau, \lambda_j \sim \mathcal{G}\left(\frac{1}{2}, \frac{1}{2\tau\lambda_j}\right), \quad \lambda_j \mid a, c \sim F(2a, 2c), \quad \tau \mid a, c \sim F(2c, 2a). \quad (8)$$

The triple gamma prior offers three key advantages. First, it is a generic choice of shrinkage prior, encompassing many well-known priors as special cases (e.g., the other global-local shrinkage priors discussed previously). Second, it is highly flexible, with the parameters  $a$  and  $c$  modifying the pole and tail behavior, respectively. Specifically, the pole around the origin becomes more pronounced as  $a$  decreases, while the tails of the distribution become heavier as  $c$  decreases. The pronounced pole effectively squelches noise, while the heavy tails allow signals to filter through. Finally, and importantly for the estimation procedure presented in Section 3, the marginal density is available in closed form:

$$f(x; a, c, \tau) = \frac{\Gamma(c + \frac{1}{2})}{\sqrt{2\pi\kappa x} B(a, c)} U\left(c + \frac{1}{2}, \frac{3}{2} - a, \frac{x}{2\kappa}\right), \quad (9)$$

where  $\kappa = \frac{2c}{\tau a}$  and  $U(a, b, z)$  is the confluent hypergeometric function of the second kind:

$$U(a, b, z) = \frac{1}{\Gamma(a)} \int_0^\infty e^{-zt} t^{a-1} (1+t)^{b-a-1} dt.$$

The closed-form marginal density simplifies the estimation procedure by reducing reliance on the full hierarchical structure of the prior, keeping the number of hyperparameters to estimate low. This computational efficiency, combined with the prior’s flexibility and generality, makes it a strong choice for high-dimensional regression tasks.

## 2.1 The Importance of Hierarchy

GPR models suffer from the curse of dimensionality in a specific way. Consider two points in the output space,  $y$  and  $y'$ . When a new covariate is added, the anisotropic distance in (4) can only increase<sup>1</sup>, leading to reduced covariance between  $y$  and  $y'$ , and, more broadly, to an increasingly sparse covariance matrix. This sparsification occurs mechanically as the number of covariates grows, even if they do not influence the outcome of interest (Binois and Wycoff, 2022). This sparsification not only affects the covariance structure but can also lead to overfitting or reduced predictive accuracy, particularly in high-dimensional settings.

The priors on  $\theta_1, \dots, \theta_d$  are critical in mitigating the curse of dimensionality by pushing the  $\theta_j$  values of irrelevant covariates toward zero, effectively excluding them. The choice of prior for the global shrinkage parameter  $\tau$  plays a particularly important role here. As shown in Cadonna et al. (2020), under the triple gamma shrinkage prior, setting  $\tau \sim F(2c, 2a)$  implies a uniform prior on the *model size*, i.e. the number of relevant covariates. This ensures that some prior mass remains on models with few or no covariates, even when  $d$  is large, while still allowing flexibility for larger models when supported by the data.

To be more precise on what "model size" means, first consider the following equivalent re-parameterization of the triple gamma prior (Cadonna et al., 2020):

$$\theta_j \mid \rho_j \sim \mathcal{G}\left(\frac{1}{2}, \frac{\rho_j}{2(1-\rho_j)}\right), \quad \rho_j \mid a, c, \tau \sim \mathcal{TPB}\left(a, c, \frac{2c}{\tau a}\right), \quad (10)$$

where  $\mathcal{TPB}$  is the three-parameter beta distribution. Importantly,  $\rho_j \in [0, 1]$  and is called the *shrinkage factor*, as it characterizes the amount of shrinkage applied to  $\theta_j$ .

This formulation generalizes the concept of shrinkage factors, well-studied in normal-means and regression settings (Carvalho et al., 2010), to positive-constrained parameters. The interpretation remains straightforward: as  $\rho_j$  approaches zero,  $\frac{\rho_j}{2(1-\rho_j)}$  approaches zero, making the prior for  $\theta_j$  converge to a gamma distribution with infinite mean and variance. Conversely, as  $\rho_j$  approaches one,  $\frac{\rho_j}{2(1-\rho_j)}$  approaches infinity, driving the prior for  $\theta_j$  toward a gamma distribution with mean and variance both zero. Thus,  $\rho_j = 1$  corresponds to total shrinkage, while  $\rho_j = 0$  implies no regularization on the parameter. Despite its origins in the sparse normal-means problem, this generalization of shrinkage factors adapts naturally to the square-transform case.

---

<sup>1</sup>Technically, it could remain constant if the associated  $\theta_j = 0$ . However, given the use of continuous shrinkage priors, this will happen with probability 0.

The shrinkage factor naturally leads to the concept of model size  $K$ , defined as the number of  $\theta_j$  where  $\rho_j < 0.5$ :

$$K = \sum_{j=1}^d \mathbb{I}(\rho_j < 0.5). \quad (11)$$

$K$  corresponds to the number of covariates that significantly contribute to the covariance matrix and is itself a random variable, with a distribution implied by the choice of hierarchical shrinkage prior:

$$K \sim \text{Binom}(d, \pi), \quad \pi = \Pr(\rho_j < 0.5). \quad (12)$$

What [Cadonna et al. \(2020\)](#) show is that under  $\tau \sim F(2c, 2a)$ , the induced probability  $\pi = \Pr(\rho_j < 0.5)$  is uniformly distributed, implying a uniform prior on the model size. This is in stark contrast to a non-hierarchical prior, where  $\pi$  is some fixed constant, a choice that is highly informative about the model size. The uniform prior ensures that models with few covariates are not overly penalized, which is critical for achieving robust performance in high-dimensional settings where irrelevant covariates dominate.

Examining the implied  $\sum_{j=1}^d \theta_j$  can serve as a measure of the *a priori* distance between observations encoded within the Gaussian process prior. This is informative, as increased distance between observations leads to a sparser covariance matrix. [Figure 2](#) shows the distribution of this measure across various  $d$  for both the hierarchical and non-hierarchical case. The hierarchical prior concentrates more mass on smaller values of  $\sum_{j=1}^d \theta_j$ , even as the covariate space increases. In contrast, the mode of the distribution under the non-hierarchical prior increases with the number of covariates, despite having the same conditional distribution. This behavior arises because the hierarchical prior induces a joint distribution over  $\theta_1, \dots, \theta_d$ , where any large  $\theta_j$  decreases the probability of other  $\theta_{-j}$  values being large.

### 3 Estimation via Normalizing Flows

Estimation of GPR models is a notoriously difficult problem, despite the log likelihood (here marginalized over the function  $f(\mathbf{x})$ ) being available in closed form:

$$\begin{aligned} \log p(\mathbf{y} \mid \tau, \theta_1, \dots, \theta_d, \sigma^2) = & -\frac{N}{2} \log(2\pi) - \frac{1}{2} \log |\mathbf{K}(\mathbf{x}; \boldsymbol{\theta}, \tau) + \sigma^2 I| \\ & - \frac{1}{2} \mathbf{y}^T (\mathbf{K}(\mathbf{x}; \boldsymbol{\theta}, \tau) + \sigma^2 I)^{-1} \mathbf{y}. \end{aligned}$$

Two main problems arise: First, the triple gamma prior is not (conditionally or otherwise) conjugate to the posterior of the hyperparameters, which precludes any closed form solutions and makes sampling based approaches less attractive. Second, the likelihood is expensive to evaluate, as it requires the inversion the  $N \times N$  matrix  $\mathbf{K}(\mathbf{x}; \boldsymbol{\theta}, \tau) + \sigma^2 I$ , which has a computational cost of order  $\mathcal{O}(N^3)$ . This problem is compounded in the fully Bayesian approach, as sampling based methods often require the likelihood to be

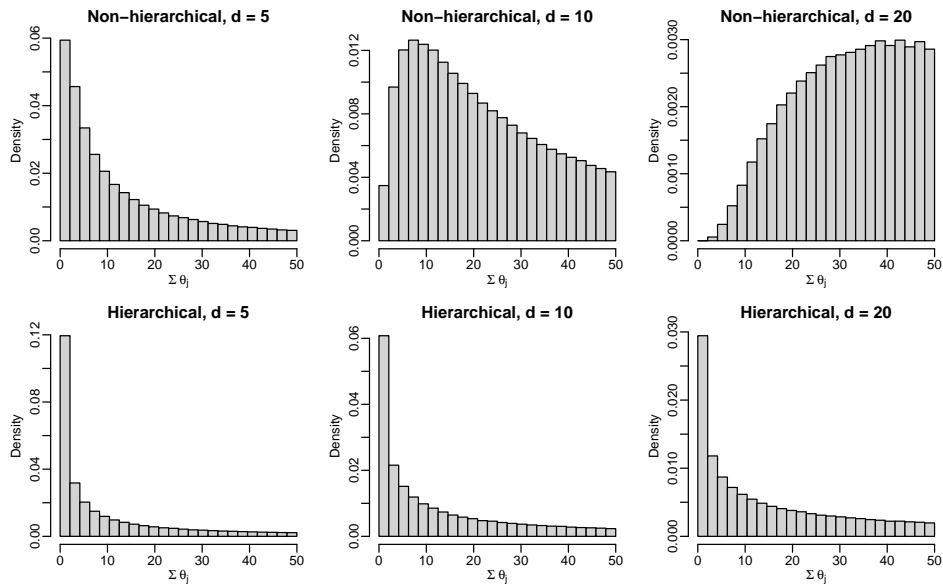


Figure 2: Samples from  $\sum_{j=1}^d \theta_j$  under the hierarchical triple gamma prior (bottom) and the non-hierarchical triple gamma prior (top), for different  $d$ . The hierarchical prior places more mass on smaller values of  $\sum_{j=1}^d \theta_j$ , even as the number of covariates increases.

evaluated at each iteration. Many widely used variational methods, such as the mean-field approximation, alleviate the computational burden but often lack expressivity, leading to poor approximations of the posterior distribution.

This work proposes a different approach to the estimation of GPR models under hierarchical shrinkage priors. Specifically, it explores the use of normalizing flows (Rezende and Mohamed, 2015) to approximate the posterior distribution in a variational inference framework. While still an approximation to the true posterior, normalizing flows are highly flexible and can approximate even complex posterior shapes in a computationally tractable way. This makes them a step up from widely used mean field approximations, which, by design, are unable to capture correlations between parameters. This may be of particular importance in a regression setting, where explanatory variables are often correlated.

The key computational advantage of normalizing flows is that the method can easily take advantage of parallelized computing available via Graphics Processing Units (GPUs). This means that a rich approximation of the posterior can be obtained, while still remaining computationally tractable. This is in contrast to sampling based approaches and other variational inference methods, where the former is inherently sequential and the latter often lacks the flexibility to capture complex posterior shapes.

### 3.1 A Brief Introduction to Normalizing Flows

Normalizing flows are a class of flexible, invertible transformations that approximate complex distributions by mapping a simple base distribution onto a more complex target distribution through a series of simpler transformations. This makes them an effective tool for variational inference, where capturing complex posterior shapes is often challenging.

To illustrate, consider the goal of defining a joint distribution over a  $D$ -dimensional random variable  $\mathbf{z}$ .<sup>2</sup> The key idea behind normalizing flows is to introduce a simple base distribution  $p_{\mathbf{u}}(\mathbf{u})$  over a random variable  $\mathbf{u}$  and then express  $\mathbf{z}$  as a transformation  $T$  of  $\mathbf{u}$ :

$$\mathbf{z} = T(\mathbf{u}), \quad \mathbf{u} \sim p_{\mathbf{u}}(\mathbf{u}).$$

Both the transformation  $T$  and the base distribution  $p_{\mathbf{u}}$  may depend on parameters, denoted here as  $\phi$  and  $\psi$ , respectively, leading to a distribution  $p(\mathbf{z}; \phi, \psi)$  over  $\mathbf{z}$ . For  $T$  to qualify as a valid flow, it must be a diffeomorphism, meaning it is invertible and both  $T$  and its inverse  $T^{-1}$  are differentiable. This constraint also requires that  $\mathbf{u}$  is of the same dimension  $D$  as  $\mathbf{z}$ . Under these conditions, the density of  $\mathbf{z}$  can be computed using the change of variables formula:

$$p_{\mathbf{z}}(\mathbf{z}) = p_{\mathbf{u}}(\mathbf{u}) |\det J_T(\mathbf{u})|^{-1},$$

where  $\mathbf{u} = T^{-1}(\mathbf{z})$  and  $J_T(\mathbf{u})$  is the Jacobian matrix of  $T$  evaluated at  $\mathbf{u}$ .

Now, consider a sequence of transformations,  $T_1, \dots, T_K$ , and define  $T$  as their composition,  $T = T_K \circ \dots \circ T_1$ . The resulting density of  $\mathbf{z}$  is then:

$$p_{\mathbf{z}}(\mathbf{z}) = p_{\mathbf{u}}(\mathbf{u}) \prod_{k=1}^K |\det J_{T_k}(\mathbf{u}_k)|^{-1},$$

where each  $T_k$  is a transformation with parameters  $\phi_k$  and  $\mathbf{u}_k$  represents the intermediate transformed variable after applying  $T_k$ . While each individual transformation  $T_k$  may be simple, the composition of them is able to approximate more complex distributions. This structure is akin to a neural network for density estimation, with each transformation acting as a “layer” subject to constraints that ensure invertibility and differentiability.

#### An Example Transformation: The Radial Flow

There exist many possible transformations that could act as individual layers in the flow, such as the planar and radial flows from the seminal paper of [Rezende and Mohamed \(2015\)](#), the Inverse Autoregressive Flow (IAF) of [Kingma et al. \(2016\)](#), or the Sylvester normalizing flow of [Berg et al. \(2018\)](#), to name a few. While they differ in their specific form, a key property they all share is that they are designed such that the Jacobian and its determinant can be computed efficiently. This is mostly achieved through the use of

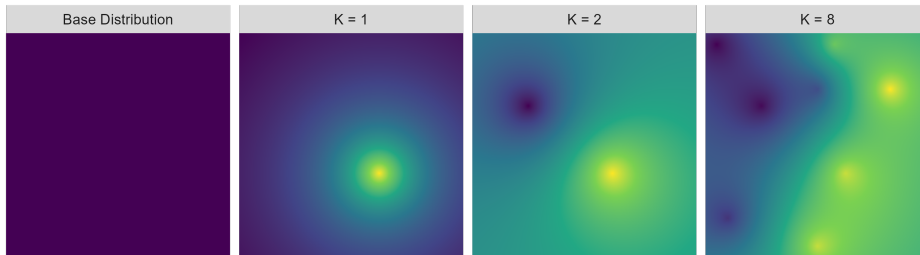


Figure 3: Effect of radial normalizing flows on a 2D uniform distribution. The base distribution (left) is progressively transformed by radial flows, introducing localized contractions or expansions around specified centers, controlled by  $\alpha$  (spread) and  $\beta$  (intensity). Density values are normalized to the range  $[0, 1]$ , with higher densities in yellow and lower densities in purple.

triangular Jacobian matrices, which have a determinant that can be computed in  $\mathcal{O}(D)$  time, where  $D$  is the dimension of the random variable one wishes to model.

To build intuition for normalizing flows, consider, as an example, the radial flow, which is defined as:

$$T(\mathbf{u}; \beta, \alpha, \mathbf{u}_0) = \mathbf{u} + \beta \frac{\mathbf{u} - \mathbf{u}_0}{\alpha + \|\mathbf{u} - \mathbf{u}_0\|_2},$$

with parameters  $\beta, \alpha, \mathbf{u}_0$ . The basic intuition behind this transformation is that it expands or contracts the base distribution around the point  $\mathbf{u}_0$ , either pushing mass towards  $\mathbf{u}_0$  or pulling it away. The spread of the contraction is controlled by  $\alpha$  and the direction and intensity is controlled by  $\beta$ . Through successive applications of this transformation, it is possible to approximate distributions that are far more complex than would appear possible at first glance. Figure 3 shows the effect of radial flows on a 2D uniform distribution, with the base distribution progressively transformed by radial flows, introducing localized contractions and expansions. Note that each layer has its own parameters  $\beta_k, \alpha_k, \mathbf{u}_{0,k}$ , leading to different transformations at each step. These are the parameters that can be learned during estimation, with the goal of approximating the posterior distribution as closely as possible.

### Normalizing Flow used in this Work

While the transformation behind the radial flow is simple and therefore good for building intuition, it suffers in terms of expressivity. As it can only contract or expand the base distribution around a single point, the number of layers  $K$  needs to be large to make the flow expressive (Papamakarios et al., 2021). As such, more complex transformations are often used in practice, as in this work, where the Sylvester normalizing flow is employed (Berg et al., 2018):

$$T(\mathbf{u}) = \mathbf{u} + \mathbf{U}\mathbf{h}(\mathbf{W}^T\mathbf{u} + \mathbf{b}),$$

<sup>2</sup>Note that, in this application, the  $\mathbf{z}$  we wish to approximate corresponds to the posterior distribution.

where  $\mathbf{U}, \mathbf{W} \in \mathbb{R}^{D \times D}$ ,  $\mathbf{u} \in \mathbb{R}^D$ ,  $\mathbf{b} \in \mathbb{R}^D$  and  $\mathbf{h}$  is an elementwise non-linear function (usually the hyperbolic tangent). It is a generalization of the planar flow of [Rezende and Mohamed \(2015\)](#) that increases the expressivity of each individual transformation. The increased expressivity of each individual layer means that fewer layers overall are required to reach the same level of expressivity.

Ensuring the transformation is invertible requires restricting the parameter space for  $\mathbf{U}$ ,  $\mathbf{W}$ , and  $\mathbf{b}$ ; see [Berg et al. \(2018\)](#) for details. It is important to note that the proposed methodology is not tied to Sylvester normalizing flows and can accommodate other transformations, if they are better suited to the problem at hand.

### 3.2 Normalizing Flows for Variational Inference

Normalizing flows’ capability to approximate complex distributions in a black-box fashion makes them well-suited for variational inference. In variational inference, the objective is to approximate the posterior distribution  $p(\boldsymbol{\xi} \mid \mathbf{y})$  by selecting the best approximation from a family of distributions  $q(\boldsymbol{\xi}; \phi)$ . This is achieved by minimizing the Kullback-Leibler (KL) divergence between the approximate distribution  $q(\boldsymbol{\xi}; \phi)$  and the true posterior  $p(\boldsymbol{\xi} \mid \mathbf{y})$ :

$$q^*(\boldsymbol{\xi}; \phi) = \arg \min_{\phi} \text{KL}(q(\boldsymbol{\xi}; \phi) \parallel p(\boldsymbol{\xi} \mid \mathbf{y})).$$

The key to using normalizing flows for variational inference is to let the family of approximating distributions  $q(\boldsymbol{\xi}; \phi)$  be defined as a normalizing flow with  $K$  transformations:

$$q(\boldsymbol{\xi}; \phi) = p_{\mathbf{u}}(\mathbf{u}) \prod_{k=1}^K |\det J_{T_k}(\mathbf{u}_k)|^{-1}.$$

where  $\phi$  now contains the parameters of each transformation  $T_k$ . Note that this is in contrast to the mean-field approximation, which assumes a factorized posterior with independent components, resulting in approximations that cannot capture dependencies. Normalizing flows, on the other hand, naturally capture dependencies within the posterior.

A common approach to minimizing the KL-divergence is by maximizing the Evidence Lower BOund (ELBO). When using normalizing flows as the approximate posterior, an ELBO of the following form arises ([Papamakarios et al., 2021](#)):

$$\text{ELBO}(\phi) = \mathbb{E}_{p_{\mathbf{u}}(\mathbf{u})} [\log p(\mathbf{y}, T(\mathbf{u}; \phi))] + \mathbb{E}_{p_{\mathbf{u}}(\mathbf{u})} [\log |\det J_T(\mathbf{u}; \phi)|]. \quad (13)$$

The reason why this approach to estimation is attractive, is that this expression can be optimized via stochastic gradient descent, which is computationally efficient and can, importantly, be run on GPUs, greatly speeding up computation.

#### Practical Considerations

While the overview given so far contains all the theory to implement normalizing flows for GPR models, a few extra comments on practical considerations may make the procedure somewhat more approachable. First, the ELBO presented in (13) is difficult to

**Algorithm 1** Normalizing Flows for Variational Inference in GPR Models

**Require:** Training data  $\mathcal{D} = \{(\mathbf{x}_i, y_i)\}_{i=1}^n$ , kernel function  $k(\cdot, \cdot; \boldsymbol{\theta}, \tau)$ , base distribution  $p_{\mathbf{u}}(\mathbf{u})$ , sequence of flow functions  $\{T_k(\cdot; \boldsymbol{\phi}_k)\}$ , number of samples  $S$  from base distribution, number of iterations  $M$

- 1: Initialize variational parameters  $\boldsymbol{\phi}_k$  for each flow layer  $k = 1, \dots, K$
- 2: **for**  $i = 1$  to  $M$  **do**
- 3:     Sample  $S$  realizations  $\{\mathbf{u}_0^{(s)}\}_{s=1}^S$  from the base distribution  $p_{\mathbf{u}}(\mathbf{u})$
- 4:     **for**  $s = 1$  to  $S$  **do**
- 5:         Initialize  $\log J^{(s)} \leftarrow 0$
- 6:         **for**  $k = 1$  to  $K$  **do**
- 7:             Apply flow transformation:  $\mathbf{u}_k^{(s)} \leftarrow T_k(\mathbf{u}_{k-1}^{(s)}; \boldsymbol{\phi}_k)$
- 8:             Update cumulative log det.:  $\log J^{(s)} \leftarrow \log J^{(s)} + \log \left| \det J_{T_k} \left( \mathbf{u}_{k-1}^{(s)}; \boldsymbol{\phi}_k \right) \right|$
- 9:             **end for**
- 10:             Apply softplus transformation:  $\boldsymbol{\theta}^{(s)} \leftarrow \text{softplus}(\mathbf{u}_K^{(s)})$
- 11:             Update cumulative log det.:  $\log J^{(s)} \leftarrow \log J^{(s)} + \log \left| \det J_{\text{softplus}} \left( \mathbf{u}_K^{(s)} \right) \right|$
- 12:         **end for**
- 13:     Approximate ELBO using Monte Carlo:

$$\text{ELBO}_{\text{MC}}(\boldsymbol{\phi}) \leftarrow \frac{1}{S} \sum_{s=1}^S \left[ \log p \left( \mathbf{y}, \boldsymbol{\theta}^{(s)} \right) + \log J^{(s)} \right]$$

- 14:     Compute gradients  $\nabla_{\boldsymbol{\phi}} \text{ELBO}_{\text{MC}}(\boldsymbol{\phi})$
- 15:     Update  $\boldsymbol{\phi}$  using a gradient ascent method
- 16: **end for**
- 17: Return optimized variational parameters  $\boldsymbol{\phi}$

compute directly, as it requires the evaluation of the expectation over the base distribution  $p_{\mathbf{u}}(\mathbf{u})$ . Therefore, in practice, the ELBO is approximated using Monte Carlo (MC) sampling. To this end,  $S$  samples  $\{\mathbf{u}_0^{(s)}\}_{s=1}^S$  are drawn from the base distribution  $p_{\mathbf{u}}(\mathbf{u})$  and transformed successively by the  $K$  flow functions to obtain  $\{\mathbf{u}_K^{(s)}\}_{s=1}^S$ , as well as the associated Jacobians  $\{\log J^{(s)}\}_{s=1}^S$ . Further, as the hyperparameters of a GPR model are all constrained to be positive, a softplus transformation  $g(x) = 1/\beta \log(1 + \exp(\beta x))$  is applied to  $\mathbf{u}_K^{(s)}$  to ensure that the parameters remain positive. This gives the current samples from the posterior approximation used for further calculations  $\boldsymbol{\xi}^{(s)} = g \left( \mathbf{u}_K^{(s)} \right)$ . Importantly, as this is also a transformation, the Jacobian of the softplus must be accounted for in the ELBO. The ELBO can then be approximated as:

$$\text{ELBO}_{\text{MC}}(\boldsymbol{\phi}) = \frac{1}{S} \sum_{s=1}^S \left[ \log p \left( \mathbf{y}, \boldsymbol{\xi}^{(s)} \right) + \log J^{(s)} \right].$$

The unnormalized log posterior  $\log p \left( \mathbf{y}, \boldsymbol{\xi}^{(s)} \right)$  evaluated at the MC samples then reads:

$$\begin{aligned} \log p(\mathbf{y}, \boldsymbol{\xi}^{(s)}) &= \log p(\mathbf{y} \mid \boldsymbol{\xi}^{(s)}) + \log p(\boldsymbol{\xi}^{(s)}) \\ &= -\frac{1}{2} \log |\mathbf{K}(\mathbf{x}; \boldsymbol{\theta}, \tau) + \sigma^2 \mathbf{I}| - \frac{1}{2} \mathbf{y}^T (\mathbf{K}(\mathbf{x}; \boldsymbol{\theta}, \tau) + \sigma^2 \mathbf{I})^{-1} \mathbf{y} \end{aligned} \quad (14)$$

$$+ \sum_{j=1}^d \frac{1}{2} (\log(\tau) - \log(\theta_j)) + \log \left( U \left( c + \frac{1}{2}, \frac{3}{2} - a, \frac{\theta_j}{2\kappa} \right) \right) \quad (15)$$

$$+ (c-1) \log(\tau) - (c+a) \log \left( 1 + \frac{c}{a} \tau \right) \quad (16)$$

$$- \lambda \sigma^2, \quad (17)$$

where (14) is the unnormalized version of the log likelihood in (13), (15) is a sum over unnormalized log densities of the triple gamma distribution in (9), (16) is the unnormalized log density of the F distribution, and (17) is the unnormalized log prior on  $\sigma^2$ , in this case assumed to be an exponential distribution.

From here, the gradients of the ELBO with respect to the parameters  $\boldsymbol{\phi}$  can be computed via backpropagation, and the parameters can be updated using a gradient ascent method (e.g., through the pytorch library; Paszke et al., 2017). The entire procedure is summarized in Algorithm 1. The loop over the samples  $S$  is written out for clarity, but, in practice, can be executed in parallel, which makes the method highly efficient and well-suited for GPU computation.

## 4 Simulation Study

To evaluate the proposed approach to GPR, a simulation study was conducted, with a particular focus on out-of-sample predictive performance. To this end, data was simulated from a GPR model, varying the following factors:

- Sparsity levels: The proportion of irrelevant covariates  $s$ , with  $s \in \{0.5, 0.6, 0.7, 0.8, 0.9\}$ .
- Dimensionality: The number of covariates  $d$ , with  $d \in \{5, 10, 25, 50\}$ .
- Sample sizes: The number of observations  $N$ , with  $N \in \{10, 50, 100, 500\}$ .

The covariates were generated as  $x_{ij} \sim \mathcal{N}(0, 1)$ , while the inverse lengthscales  $\theta_1, \dots, \theta_d$  were drawn from a noncentral chi-squared distribution with 1 degree of freedom and a noncentrality parameter of  $1.5^2$ . This strikes a nice balance of ensuring the  $\theta_j$  are different enough from 0 to be detected, while not having individual  $\theta_j$  being so large they dominate the covariance structure. Of the  $d$   $\theta_j$ ,  $\lfloor s \cdot d \rfloor$  were randomly set to 0. The response variable was then generated as  $\mathbf{y} \sim \mathcal{N}(\mathbf{0}, \mathbf{K}(\mathbf{x}; \boldsymbol{\theta}, \tau) + 0.1\mathbf{I})$ , where  $\mathbf{K}(\mathbf{x}; \boldsymbol{\theta}, \tau)$  is the covariance matrix generated by the squared exponential kernel with parameters  $\boldsymbol{\theta}$  and  $\tau$ .

The proposed normalizing flow approach was compared to a standard GPR model with an ARD kernel, estimated using a maximum likelihood (ML) approach with the GPy library (GPy, since 2012), as well as a mean-field variational approximation implemented in rstan (Stan Development Team, 2024). For the ML method, optimization

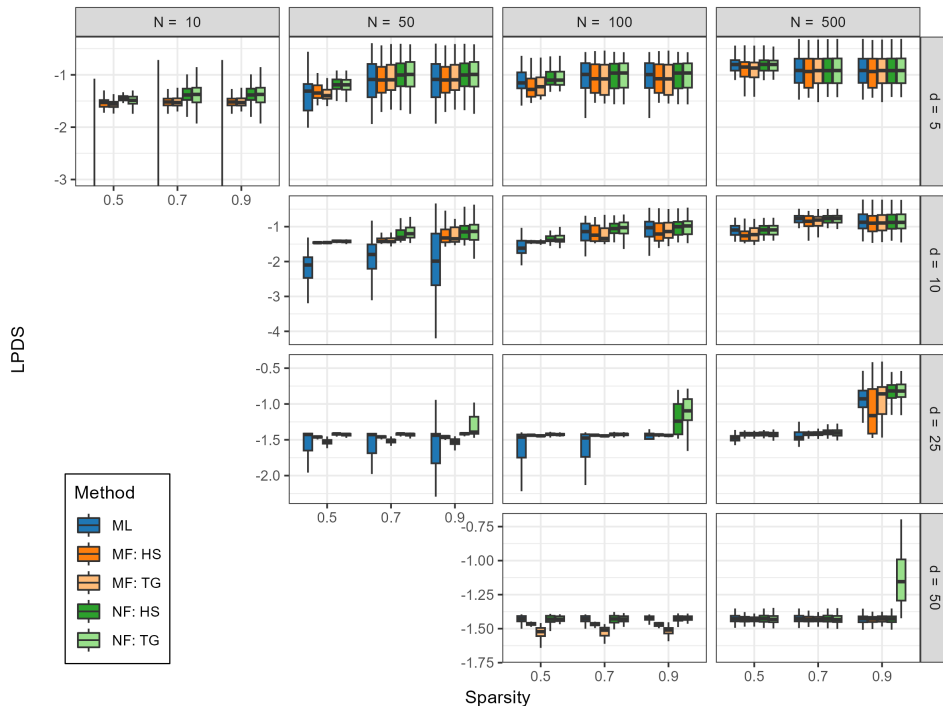


Figure 4: Log Predictive Density Scores (LPDS) for Maximum Likelihood (ML), mean-field (MF) approximation under a horseshoe (MF: HS) and triple gamma prior (MF: TG) and the proposed approach under a horseshoe prior (NF: HS) and triple gamma prior (NF: TG) across varying sparsity levels, sample sizes ( $N$ ), and dimensions ( $d$ ). NF methods outperform ML and MF, especially at higher sparsity and dimensionality, with NF: TG showing strong robustness, especially in high sparsity settings. Y-axes are scaled per row.

was restarted 10 times, with the best result retained. For the mean-field approximation, convergence was assessed by ensuring that the relative norm of the objective was smaller than 0.01, the default setting in rstan.

For both the proposed method and the mean-field approximation, two prior specifications were considered: one with  $a = c = 0.1$  and another with  $a = c = 0.5$ . The former represents a more aggressive triple gamma specification, with strong shrinkage near the origin and very heavy tails, while the latter corresponds to the horseshoe prior of [Carvalho et al. \(2010\)](#). In both cases,  $\tau \sim F(2c, 2a)$  and  $\sigma^2 \sim \text{Exp}(10)$ . The approximating flows consisted of 10 layers, and 10 latent samples were used for each Monte Carlo estimate of the ELBO. The normalizing flow models were run for 3000 iterations to ensure convergence, although this was typically achieved much earlier.

Each configuration was repeated across 50 independent runs. For each run, the data

was split into a training set (of size  $N$ ) and a test set of 300 observations. Performance was evaluated using the average log predictive density score (LPDS) on the test set, with higher LPDS values indicating better predictive performance.

The results are presented in Figure 4. Generally, the proposed normalizing flow approach outperforms both the ML and mean field method, especially at higher sparsity levels and dimensions, although all methods perform comparatively when the ratio of data points to covariates is high. Even when performing equally well in terms of the median LPDS, the ML and mean field approach often displays higher variability, potentially indicating that it is less robust in estimating predictive densities. The triple gamma prior, with its aggressive shrinkage and heavy tails, performs particularly well in high sparsity settings, while still being competitive in lower sparsity settings. It is important to note that the cost for this increased predictive performance is a higher computational burden. While the normalizing flow approach is computationally efficient *for a fully Bayesian approach*, it still remains significantly slower than the ML approach.

## 5 Concluding Remarks and Outlook

This work has contributed to the literature on Gaussian Process Regression (GPR) in two key ways. First, hierarchical shrinkage in the form of the hierarchical triple gamma prior was investigated as a mechanism to mitigate the curse of dimensionality in high-dimensional regression settings. The prior demonstrated the ability to effectively exclude irrelevant covariates while maintaining flexibility in model size. Second, a novel approach to estimating GPR models was introduced, leveraging normalizing flows within a variational inference framework. This approach enables the approximation of complex posterior distributions in a computationally efficient manner, capitalizing on advances in GPU computing. The proposed methodology outperformed a standard maximum likelihood-based approach in simulation studies, particularly in settings characterized by high dimensionality and sparsity.

The use of normalizing flows for posterior approximation remains a relatively novel concept in the context of GPR models, and there are several promising avenues for future research. First, the choice of transformation is critical to the method’s performance, and exploring alternatives such as the Inverse Autoregressive Flow (Kingma et al., 2016) could yield further improvements. Recent studies, including Kong and Chaudhuri (2020), suggest that Sylvester flows may lack the expressivity of other options, underscoring the potential benefits of investigating more flexible transformations. Second, while the methodology is currently able to scale to datasets of reasonable size, extending it to sparse GPR models (see, e.g., Quinonero-Candela and Rasmussen, 2005, for an overview) could enable its application to truly large datasets. However, such an extension would need to address the computational challenges associated with estimating a large number of inducing points, which would significantly increase the dimension of the posterior, thereby also increasing the size of the approximating normalizing flow. Finally, extending the approach to non-Gaussian outcomes may be of interest. The absence of a closed-form marginalized likelihood in this setting would necessitate inference

of the latent function  $f(\mathbf{x})$ , increasing posterior dimensionality and potentially reducing computational efficiency. These challenges notwithstanding, the proposed methodology offers a promising foundation for future research in GPR estimation.

### Funding

This research was funded in whole or in part by the Austrian Science Fund (FWF) 10.55776/J4806.

## References

- Alexanderian, A. (2015). “A brief note on the Karhunen-Loève expansion.” *arXiv preprint arXiv:1509.07526*. 2
- Berg, R. v. d., Hasenclever, L., Tomczak, J. M., and Welling, M. (2018). “Sylvester normalizing flows for variational inference.” *arXiv preprint arXiv:1803.05649*. 9, 10, 11
- Binois, M. and Wycoff, N. (2022). “A survey on high-dimensional Gaussian process modeling with application to Bayesian optimization.” *ACM Transactions on Evolutionary Learning and Optimization*, 2(2): 1–26. 6
- Cadonna, A., Frühwirth-Schnatter, S., and Knaus, P. (2020). “Triple the gamma – A unifying shrinkage prior for variance and variable selection in sparse state space and TVP models.” *Econometrics*, 8(2): 20. 5, 6, 7
- Carvalho, C. M., Polson, N. G., and Scott, J. G. (2009). “Handling sparsity via the horseshoe.” *Journal of Machine Learning Research W&CP*, 5: 73–80. 5
- (2010). “The horseshoe estimator for sparse signals.” *Biometrika*, 97(2): 465–480. 2, 6, 14
- Chen, T. and Wang, B. (2010). “Bayesian variable selection for Gaussian process regression: Application to chemometric calibration of spectrometers.” *Neurocomputing*, 73(13-15): 2718–2726. 2
- Frühwirth-Schnatter, S. and Wagner, H. (2010). “Stochastic model specification search for Gaussian and partial non-Gaussian state space models.” *Journal of Econometrics*, 154(1): 85–100. 5
- George, E. I. and McCulloch, R. E. (1993). “Variable Selection via Gibbs Sampling.” *Journal of the American Statistical Association*, 88(423): 881–889. 2
- (1997). “Approaches for Bayesian Variable Selection.” *Statistica Sinica*, 7(2): 339–373. 2
- GPy (since 2012). “GPy: A Gaussian process framework in python.” <http://github.com/SheffieldML/GPy>. 13
- Griffin, J. E. and Brown, P. J. (2010). “Inference with Normal-Gamma prior distributions in regression problems.” *Bayesian Analysis*, 5(1): 171–188. 5

- Kingma, D. P., Salimans, T., Jozefowicz, R., Chen, X., Sutskever, I., and Welling, M. (2016). “Improved variational inference with inverse autoregressive flow.” *Advances in neural information processing systems*, 29. [9](#), [15](#)
- Kong, Z. and Chaudhuri, K. (2020). “The expressive power of a class of normalizing flow models.” In *International conference on artificial intelligence and statistics*, 3599–3609. PMLR. [15](#)
- Legramanti, S., Durante, D., and Dunson, D. B. (2020). “Bayesian cumulative shrinkage for infinite factorizations.” *Biometrika*, 107(3): 745–752. [2](#)
- Liu, X. and Guillas, S. (2017). “Dimension Reduction for Gaussian Process Emulation: An Application to the Influence of Bathymetry on Tsunami Heights.” *SIAM/ASA Journal on Uncertainty Quantification*, 5(1): 787–812. [2](#)
- Mitchell, T. J. and Beauchamp, J. J. (1988). “Bayesian Variable Selection in Linear Regression: Rejoinder.” *Journal of the American Statistical Association*, 83(404): 1035. [2](#)
- Neal, R. M. (1996). *Bayesian Learning for Neural Networks*. Springer New York, NY. [1](#)
- Paananen, T., Piironen, J., Andersen, M. R., and Vehtari, A. (2019). “Variable selection for Gaussian processes via sensitivity analysis of the posterior predictive distribution.” In *The 22nd international conference on artificial intelligence and statistics*, 1743–1752. PMLR. [2](#)
- Papamakarios, G., Nalisnick, E., Rezende, D. J., Mohamed, S., and Lakshminarayanan, B. (2021). “Normalizing flows for probabilistic modeling and inference.” *Journal of Machine Learning Research*, 22(57): 1–64. [10](#), [11](#)
- Park, C., Borth, D. J., Wilson, N. S., and Hunter, C. N. (2022). “Variable selection for Gaussian process regression through a sparse projection.” *IJSE Transactions*, 54(7): 699–712. [2](#)
- Park, T. and Casella, G. (2008). “The Bayesian Lasso.” 103(482): 681–686. [5](#)
- Paszke, A., Gross, S., Chintala, S., Chanan, G., Yang, E., DeVito, Z., Lin, Z., Desmaison, A., Antiga, L., and Lerer, A. (2017). “Automatic differentiation in pytorch.” [13](#)
- Piironen, J. and Vehtari, A. (2016). “Projection predictive model selection for Gaussian processes.” In *2016 IEEE 26th International Workshop on Machine Learning for Signal Processing (MLSP)*. IEEE. [2](#)
- Polson, N. G. and Scott, J. G. (2011). “Shrink Globally, Act Locally: Sparse Bayesian Regularization and Prediction.” In *Bayesian Statistics 9*, 501–538. Oxford University Press. [4](#)
- Quinero-Candela, J. and Rasmussen, C. E. (2005). “A unifying view of sparse approximate Gaussian process regression.” *The Journal of Machine Learning Research*, 6: 1939–1959. [15](#)

- Rasmussen, C. E. and Williams, C. K. I. (2005). *Gaussian Processes for Machine Learning*. The MIT Press. 3
- Rezende, D. and Mohamed, S. (2015). “Variational inference with normalizing flows.” In *International conference on machine learning*, 1530–1538. PMLR. 2, 8, 9, 11
- Savitsky, T., Vannucci, M., and Sha, N. (2011). “Variable Selection for Nonparametric Gaussian Process Priors: Models and Computational Strategies.” *Statistical Science*, 26(1). 2
- Stan Development Team (2024). “RStan: the R interface to Stan.” R package version 2.32.6.  
URL <https://mc-stan.org/> 13
- Tang, T., Mak, S., and Dunson, D. (2024). “Hierarchical Shrinkage Gaussian Processes: Applications to Computer Code Emulation and Dynamical System Recovery.” *SIAM/ASA Journal on Uncertainty Quantification*, 12(4): 1085–1112. 2
- Tripathy, R., Bilonis, I., and Gonzalez, M. (2016). “Gaussian processes with built-in dimensionality reduction: Applications to high-dimensional uncertainty propagation.” *Journal of Computational Physics*, 321: 191–223. 2
- van der Vaart, A. W. and van Zanten, J. H. (2009). “Adaptive Bayesian estimation using a Gaussian random field with inverse Gamma bandwidth.” *The Annals of Statistics*, 37(5B). 1
- Vo, G. and Pati, D. (2017). “Sparse Additive Gaussian Process with Soft Interactions.” *Open Journal of Statistics*, 07(04): 567–588. 2
- Yan, F. and Qi, Y. (2010). “Sparse Gaussian process regression via  $\ell_1$  penalization.” In *Proceedings of the 27th International Conference on Machine Learning (ICML-10)*, 1183–1190. Citeseer. 2
- Yi, G., Shi, J. Q., and Choi, T. (2011). “Penalized Gaussian Process Regression and Classification for High-Dimensional Nonlinear Data.” *Biometrics*, 67(4): 1285–1294. 2